Generation of streamwise vortices in square sudden-expansion flows

Amalendu Sau*
48-121 Engineering IV Building, Department of Mechanical and Aerospace Engineering, University of California, Los Angeles, California 90095-1597, USA

(Received 1 July 2003; revised manuscript received 1 December 2003; published 24 May 2004)

The intent of the present work is to investigate the nature of jet spreading and the process of evolution of the associated embedded streamwise vortices for the steady flow through a two-step square sudden expansion. Simulations are performed to review the flow physics within a square channel which undergoes a first expansion with an uniform step height 0.75*h* (*h* being the inlet channel width); and at a streamwise distance 8*h* from the plane of first expansion the channel goes through another expansion with the second step height being half of the first step height. Unlike asymmetric jets, the square jet is observed to experience relatively faster nonuniform azimuthal perturbations during its streamwise evolution and at some downstream location the jet expands in such a way that it looks as if it has locally rotated by 45°. The developed four pairs of outflow type streamwise vortices (with each pair occupying their position at the end of a jet diagonal), which dominated over the first expansion zone, seems to control the azimuthal jet deformation process through their induced outward velocity. Another important aspect of the present investigation is that here we have established a unique pressure analysis which efficiently predicts the presence of all the streamwise vortices in the setup and also their nature of dynamics without any ambiguity. Moreover, the presented pressure analysis suggests that nonuniform lateral flow acceleration within the channel, as induced by the developed transverse pressure gradient skewing, influences the generation of the streamwise vortices. The pressure analysis also successfully predicts every local change in the dynamics of the embedded streamwise vortices, during the downstream evolution of the jet.

DOI: 10.1103/PhysRevE.69.056307 PACS number(s): 47.15.−x, 47.27.Wg, 47.32.Cc

I. INTRODUCTION

Recent investigations (e.g., Liepmann and Gharib [1], Zaman [2], Sau [3]) concerning the flow physics involved in the processes of entrainment and mixing with various jets demonstrate the important role played by the dynamics of the embedded streamwise vortices. Moreover, small aspect-ratio jets are known (e.g., Husain and Hussain [4], Ho and Gutmark [5], Hertzberg and Ho [6,7] to possess significantly higher mass entrainment and mixing ability, compared to those with large aspect ratio. Notably, recent findings on the topic (e.g., Zaman [2] and Sau [3,8,9]) reveal that, through the inflow type dynamics, a pair of streamwise extended vortical rollers continue to entrain the ambient fluid into the jet core. On the other hand, a pair of outflow type streamwise vortices essentially ejects the jet core fluid outward. The dynamics of the embedded streamwise vortices thereby effectively controls the mixing process. Furthermore, the existing experimental (e.g., duPlessis *et al.* [10], Quinn and Militzer [11], Quinn [12]) and the computational (e.g., Sau [8], Grinstein *et al.* [13], Grinstein and DeVore [14]) studies concerning the vortical flow development with square jets also demonstrate the continued dominance of streamwise vortices in the flow field. In the near field, a square jet is known to experience relatively quick azimuthal perturbations during its streamwise evolution. Owing to the faster spreading along the two principle axes of symmetry, the jet expands in such a way that at some downstream location the jet section gets deformed into another square shape with its two diagonals rotated (e.g., Sau [8], Quinn [12], Grinstein *et al.* [13], Grinstein and DeVore [14]) by 45 °. Importantly, such an azimuthal deformation process of a square jet is observed to take place both for laminar as well as turbulent flows. On the other hand, the associated process of nonuniform azimuthal jet perturbations for asymmetric (elliptic or rectangular) jets lead to the 90° axis switching of the jet section (e.g., Ho and Gutmark [5], Zaman [2], Sau [8]) at some downstream location. Notably, as far as the role of streamwise dynamics in the downstream jet deformation process is concerned, recent findings by Zaman [2] and Sau [3,8,9] clearly demonstrate the fact that the streamwise vortices effectively control such jet perturbation processes through their induced inward and outward velocities. Furthermore, existing experimental observations reveal that even slight changes in the local curvature variation of a physical setup can lead to the generation of a totally different type of streamwise vortex structure. For example, for flows through a duct transitioning from a circular to a rectangular cross section, Davis and Gessner [15] observed the presence of two pairs of inflow type streamwise vortices at the ends of the major axis of their physical setup. Whereas, for flow through a similar transitioning duct with only a minor difference in the gradual cross-sectional change in the duct geometry, the experiments conducted by Miau *et al.* [16] produced outflow type streamwise vortices. In addition, the recent simulations of flows through channels with rectangular sudden expansion and contraction, as presented by Sau [3, 8], reveal that even passive forcing-induced local generation/dissipation of the streamwise vortices can totally change the nature of the dynamics of the dominant stream-

*Present address: Institute of Physics, Academia Sinica, Nankang 11529, Taipei, Taiwan. Electronic address: asau@phys.sinica.edu.tw

wise vortices during their downstream evolution.

Remarkably, despite several experimental and theoretical efforts, the source of generation of these technically important streamwise vortices and the related flow physics in most of the physical systems remained more or less unknown. A closer review of the existing literature (e.g., Zaman [2], Sau [3,9], Bradshaw [17], Kim and Samimy [18]) on the topic, however, suggests that the skew-induced generation process (i.e., Prandtl's first kind of secondary flow) may be the possible source of the streamwise vortices for the class of flows just discussed. The developed spanwise pressure gradient within the channel is believed to influence the growth and the sustained evolution process of the streamwise vortices. On the other hand, viscous stresses will cause streamwise vortices to decay. Such predictions hold good both for the vortices which remain distributed through the shear layer, as in a conventional 3D boundary layer, or for those concentrated into identifiable streamwise vortices. To this point, recently conducted direct numerical simulation (DNS) studies for the asymmetric sudden expansion flows, as presented by Sau [3,9], shed some light into the physical process and suggest that the developed transverse pressure gradient plays the crucial role in the generation process of streamwise vortices. However, for turbulent flows the streamwise mean vorticity can also be generated by the Reynolds stress (i.e., Prandtl's second kind of secondary flow being the major source), but such stress-induced generation usually contributes to the development of much weaker vortices (e.g., Bradshaw [17]). On the other hand, for supersonic jets the developed baroclinic torque, formed due to misalignment of the pressure and the density gradients, can lead to the generation of the streamwise vortices (e.g., Kim and Samimy [18]). Such misalignment of the pressure and the density gradients in hypersonic flows usually takes place due to the generated local heating at high velocities, resulting in a significant temperature variation within the flow field.

Notably, in a couple of recent computational studies Sau [3,9] attempted to investigate the source of generation of the streamwise vortices for rectangular sudden expansion/contraction flows and performed a detailed pressure analysis. The pressure distribution for such flows reveals the development of several relative high and low pressure regions within the physical domain, leading to the generation of a significant transverse pressure gradient on every cross-stream channel section. The detailed pressure analysis as presented in Refs. [3] and [9] also indicates that the nonuniform lateral flow acceleration from the high pressure regions to the neighboring low pressure regions, as induced by the developed skewed transverse pressure gradient, is the primary reason behind generation of the streamwise vortices. Since the nature of dynamics of the embedded streamwise vortices and the associated process of azimuthal jet perturbations through the square sudden expansions (e.g., Sau [8], Quinn [12]) are entirely different from what one usually encounters with rectangular jets, and since the presence of a second expansion in the setup (Fig. 1) causes the generation of passive-forcing-induced new streamwise vortices, the objective of the present brief study is to investigate both the nature of downstream jet spreading and the process of generation of the embedded streamwise vortices for the steady flow through a two-step square sudden expansion, and to examine whether the pressure analysis, as recently proposed by Sau [3,9], can be successfully extended to identify the streamwise vortices in the present setup as well.

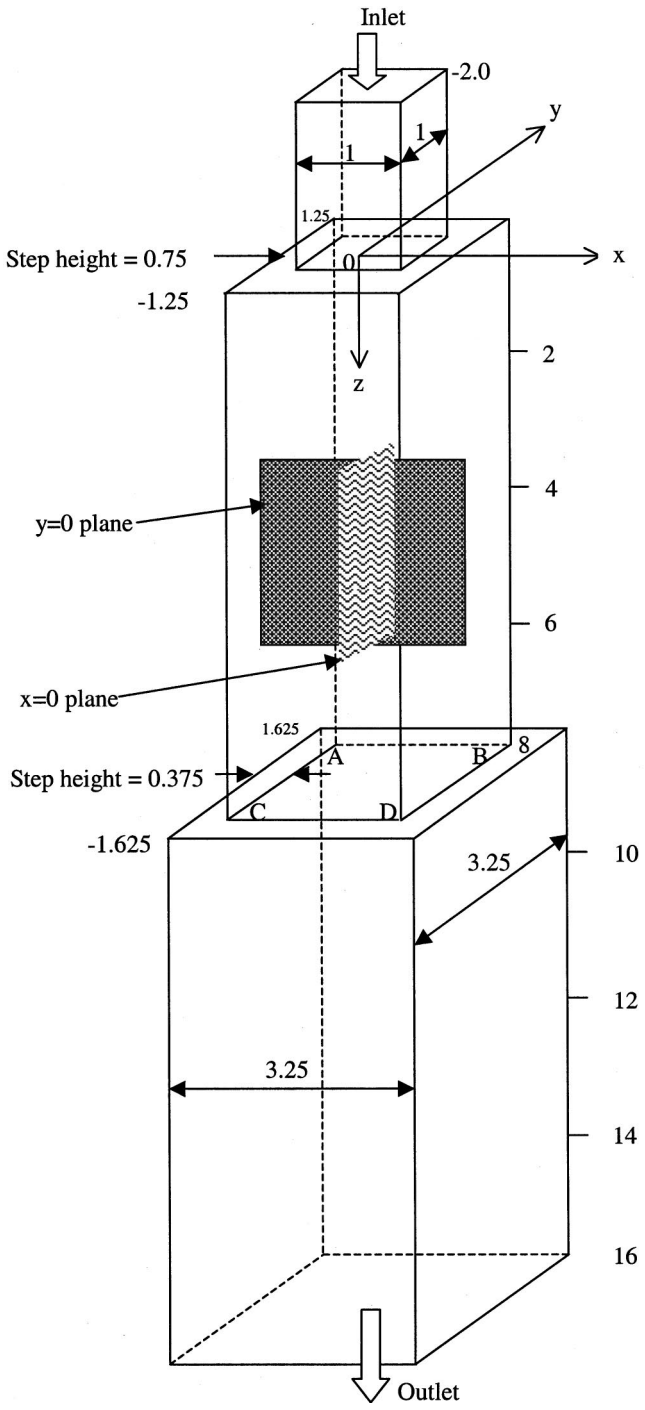

FIG. 1. Schematic representation of the physical setup.

II. GOVERNING EQUATIONS AND BOUNDARY CONDITIONS

Details of the incompressible laminar flow through a square sectioned channel with two consecutive steps of sud-

den expansions (Fig. 1) were obtained by numerically solving the following nondimensional equations in three dimensions:

$$D \equiv \nabla \cdot \underline{u} = 0, \tag{1}$$

$$\underline{u}_t + \underline{u} \cdot \nabla \underline{u} = -\nabla p + \frac{1}{Re}\nabla^2 \underline{u}. \tag{2}$$

We use Cartesian coordinates (x,y,z) with corresponding velocity components (u,v,w), and p is the pressure. Here all lengths have been nondimensionalized with respect to the channel width h upstream of the expansion, the velocities are normalized with respect to the average incoming velocity $\overline{w}$ at the channel inlet, and the pressure with respect to $\rho\overline{w}^2$. The Reynolds number for the flow is defined as $\mathrm{Re}=\overline{w}h/\nu$.

As an appropriate closure boundary condition, a fully developed axial velocity profile (e.g., White [19]) with unit mean was implemented at the channel inlet, which is situated at a non-dimensional distance 2, above the plane of first expansion (Fig 1). Other velocity components at the inlet are set to zero so that any possibility of inlet swirling is avoided. On the surrounding rigid surfaces, the no-slip wall boundary conditions, $\underline{u}=0$, are used, and the zero gradient outflow conditions were implemented at the channel exit. Simulations are conducted in a domain with nondimensional axial lengths $X_{max}=Y_{max}=1.625$ and $Z_{max}=16.0$.

III. METHOD OF SIMULATION

The governing system of Eqs. (1) and (2) in the primitive variables were discretized using a staggered control volume method in order to solve for $\underline{u}$ and p. In the interior of the computational domain, the convective terms are discretized by using a third-order accurate quadratic upwind interpolation for convective kinematics (QUICK) scheme, whereas the viscous terms are discretized using a fourth-order accurate central difference scheme. Near the wall boundaries, second-order accurate central difference methods are used in order to discretize the convection and the viscous terms. Details of the implemented computational schemes are provided in our recent works on the topic (e.g., Sau [9] and Sau *et al.* [20]). While most of the terms in the momentum equations were explicitly approximated, the coupling between pressure and velocities was implicit. The discretized semi-implicit algebraic system of equations was solved using the successive over-relaxation (SOR) method in order to accelerate convergence. An improved version of the Marker-and-Cell (MAC) method of Harlow and Welch [21] is implemented to solve the discretized system, where velocity components are advanced explicitly to take into account the combined effect of convection, diffusion and pressure gradients, and the adjustment between pressure and velocity is done iteratively in order to control the mass balance in each cell. Notably, the present iterative method is equivalent to correcting the pressure field from the Poisson equation. The iterative process is then repeated successively until the sum of discrete divergence, D, of velocities in all the cells became smaller than 10^{-4}. Among others in recent years, Sau [3,8,9], Sau *et al.* [20], Chiang *et al.* [22], Sau and Lahiri [23] and Peng *et al.* [24] have successfully implemented the computational scheme while solving various fluid dynamic problems. A spatial resolution of $63\times63\times326$ grid points were used to discretize the flow domain and each simulation took about 900 hours of CPU time on a 2 GHz PENTIUM IV processor. To ensure the accuracy of the presented results, several grid independence studies are conducted during the course of experimenting with the flow simulation, and the optimum grid resolution is used.

IV. RESULTS AND DISCUSSION

In order to improve our understanding about the flow physics and to demonstrate the consistency of the presently simulated results with recent experimental and theoretical predictions, it is important that we present the details of the jet deformation process and the associated dynamics of the embedded streamwise vortices, before we focus our attention toward investigating the generation mechanism of the streamwise vortices.

A. Process of jet deformation and the associated streamwise dynamics

The depicted representative isovelocity (w) contours in the first two columns of Fig. 2(a) display the gradual azimuthal deformation the jet experiences during its streamwise evolution, starting immediately behind the plane of first expansion. The Reynolds number for the flow, based on the average inlet velocity and the width of the inlet channel, is taken as 300. Quite expectedly, the jet structure slightly ($z=0.05$) below the plane of first expansion preserves its upstream square shape. Then, a relatively quick nonuniform azimuthal perturbation of the jet is observed to take place. Due to its rapid expansion along the x and y axes, the deformed shape of the jet section on $z=1$ looked as if the entire jet at this location has rotated by 45°, and consequently two diagonals of the jet have also rotated by the same angle. Such a structural deformation of the jet was observed to continue through $1\leqslant z\leqslant 6$, and as the jet approached the end of the first expansion zone, it gradually took a circular shape. In order to better understand the azimuthal deformation process of the jet immediately behind the plane of expansion $z=0$, in Fig. 2(b) we present the evolution of an isosurface of the w velocity. Figure 2(b) clearly shows that the jet upon leaving the plane of expansion ($z=0$) quickly expands along the x and y axes, and the magnitude of such expansion is maximum [see also the isocontours of w in Fig. 2(a)] on the two principle planes of symmetry. Later we shall explain how the dynamics of the locally grown streamwise vortices initiates such a centrosymmetric deformation process of the jet with respect to the channel geometry. As far as the observed jet deformation process [Fig. 2(a), columns 1 and 2] is concerned, here we may mention that our findings in this regard remained very much consistent with the experimental observations as reported by Quinn [12] and the simulated results of Grinstein *et al.* [13]. As the jet crossed the plane of second expansion ($z=8$), there occurred an additional azimuthal jet

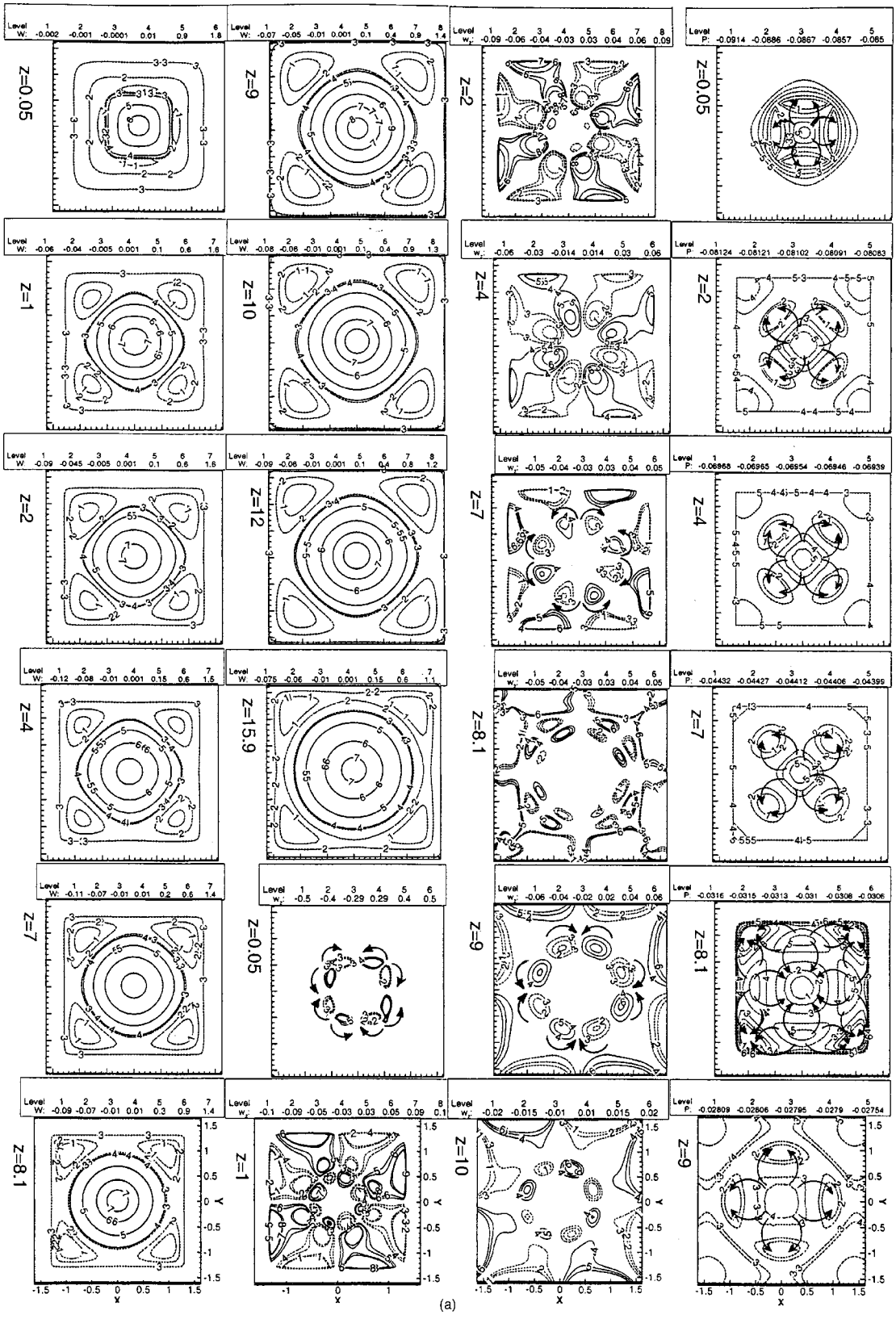

FIG. 2. (a) Contours of the streamwise velocity (w), streamwise vorticity (ω_z), and the dynamic pressure (p) at $Re=300$. (b) An isosurface of streamwise velocity (w), demonstrating the 3D evolution of the jet at $Re=300$. (c) 3D evolution pattern of the streamwise (ω_z) vortices inside the channel at $Re=300$. (d) Streamwise flow evolution on the symmetry plane $y=0$ and on $y=0.49$ at $Re=300$.

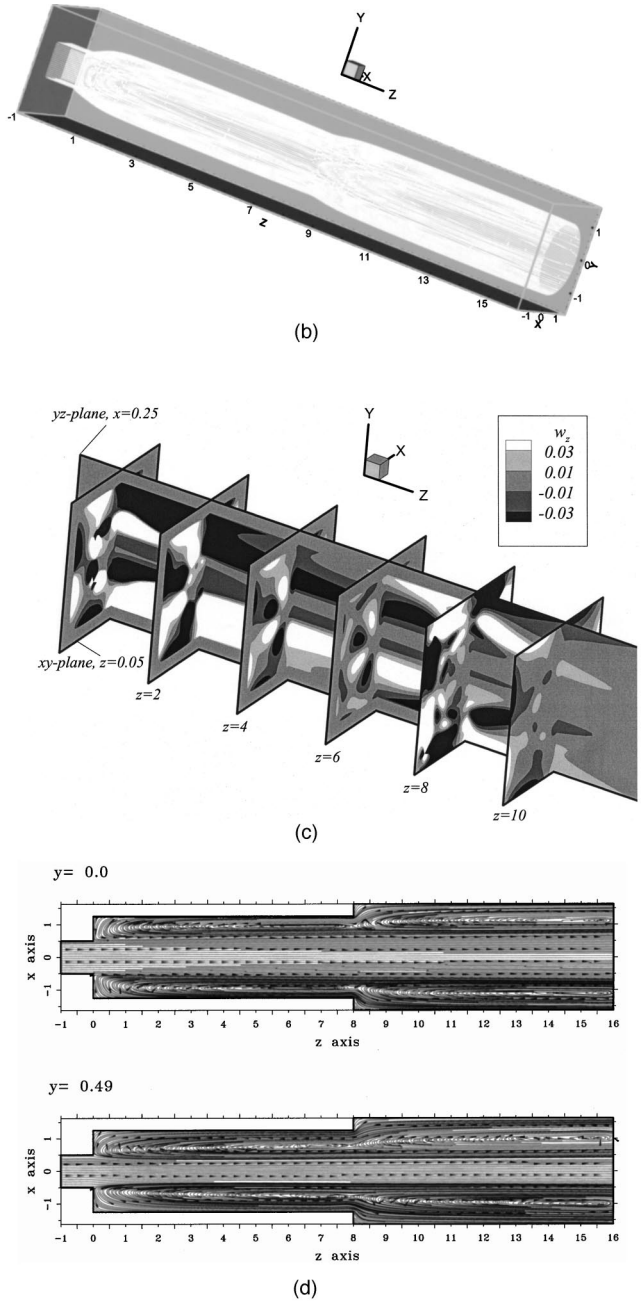

FIG. 2. (*Continued*).

perturbation within $9 \leqslant z \leqslant 12$, which apparently forced the jet to locally retain its 45° rotated square shape, before it took the eventual circular form while approaching the channel exit. Notably, the dotted isocontours of the streamwise velocity w, surrounding the corresponding solid contours [Fig. 2(a), columns 1 and 2], display the structure of the upstream recirculating flow zone. They reveal the fact that, there always remain present the symmetrically developed upstream flow along the surrounding walls, which virtually enveloped the downstream moving jet.

The sectional streamwise vorticity (ω_z) distribution for the flow is presented towards the end of the second column and in the third column of Fig. 2(a). Notably, the vorticity dynamics on $z=0.05$, as indicated by arrows with the contours, reveal the generation of four pairs of outflow type streamwise vortices from the four sharp inner edges on the plane of first expansion. The important development that may be noted here is that, within $1 \leqslant z \leqslant 4$, the vorticity contours display a rapid growth of passive forcing induced wall vortices starting immediately behind the plane of first expansion [see also Fig. 2(c)]. The wall vortices at this location are seen to quickly grow stronger at the expense of the gradually decaying core streamwise vortices, and by $z=2$ the core vortices have dissipated. These wall vortex turned streamwise vortices are seen to dominate over the entire first expansion zone, where they grouped themselves symmetrically into four outflow type pairs with each pair securing its position at the end of a diagonal of the 45° rotated jet. Moreover, the depicted arrows with the streamwise vorticity (ω_z) contours on $z=7$ clearly indicate the presence of four pairs of outflow type streamwise vortices at the ends of the x and y axes. From vorticity dynamics we know that such pairs of streamwise vortices, through their induced outward velocity, will move away from the jet centre along the x and y axes and will eject the core fluid out through the ends of the principle axes. In this way streamwise vortices play an active role in enhancing the mixing between the core fluid and the ambient fluid. Here we may mention that the streamwise vortices in the Quinn's [12] experiment, dealing with turbulent square jet flows, are observed to change their orientation from inflow to outflow type. However, the streamwise vortices for the presently investigated steady laminar flow through a square channel with two consecutive steps of sudden expansion are seen to maintain their outflow type dynamics through the first expansion zone, and later over the second expansion zone the dominant vortices become of inflow type. In view of previous experimental observations reported by Davis and Gessner [15] and Miau *et al.* [16], it appears that such differences in the orientation of the streamwise vortices are not uncommon and are usually attributed to the geometry of upstream flow. On the other hand, over the first expansion zone, the presently simulated overall nature of dynamics of the embedded streamwise vortices remained very much consistent with the streamwise dynamics for the corresponding single step sudden expansion flow, as reported by Sau [8]. Notably, from the distribution of the streamwise vortices [Fig. 2(a), columns 2 and 3] within $1 \leqslant z \leqslant 7$, it appears that the induced outward motion of the four pairs of streamwise vortices, situated at the ends of the x and y axes, influenced the jet to expand symmetrically and equally along the principle axes, and thereby controlled the azimuthal deformation of the jet, leading to its apparent 45° rotation. At this point it may be noted that, unlike rectangular jets (e.g., Zaman [2], Sau [3,9]), the developed streamwise vortices surrounding a square jet remained relatively weak, and with streamwise evolution they lose their strength at a faster rate. As a result, the jet also quickly became circular. It will be shown later that the developed lateral pressure gradient plays an important and decisive role in the generation as well as in the downstream evolution process of the streamwise vortices. Notably, besides the presence of four pairs of streamwise vortices emerging from the first expansion zone into the second expansion zone, the streamwise vorticity contours on $z=8.1$ [Fig. 2(a), column 3] reveal the presence of four addi-

tional pairs of streamwise vortices which are generated from the four inner edges (A,B,C,D, as indicated in Fig. 1) on the plane of second expansion. The persisting inner four outflow type pairs of streamwise vortices, however, are seen to become quickly dissipated. Moreover, as the vorticity contours on $z=9$ and 10 reveal, the inflow type outer pairs (as represented by arrows with the vorticity contours on $z=9$), which are generated from the four inner edges on the plane of second expansion, also survive only a short distance and eventually become dissipated just behind the plane $z=10$ [see also Fig. 2(c)]. Here we would like to mention that, unlike in asymmetric (rectangular) jets, the existing experimental (e.g., Quinn [12]) and the simulated results (e.g., Sau [8]) reveal that the streamwise vortices for the square jet dominate within a comparatively short distance and then dissipate very quickly. As a consequence the jet also experiences a relatively faster azimuthal deformation (see also Grinstein *et al.* [13]) leading to a quick 45° rotation of the downstream jet structure, before taking the eventual circular shape.

In order to provide a better understanding concerning the growth of the streamwise vortices in the setup, in Fig. 2(c) we demonstrate their more complete 3D evolution details. Notably, a combined view of Fig. 2(a) and 2(c) reveals that the initial streamwise (ω_z) vortices, those generated from the sharp inner edges on the plane of first expansion, entirely dissipate by $z=2$, and the fast growing passive forcing induced wall vortices quickly take over to dominate the downstream flow in the first expansion zone. Then, as the flow enters the second expansion zone, one observes the growth of additional vortices generated from the inner edges on the plane of second expansion. While the transmitted inner vortices are seen to dissipate soon after $z=8$, the streamwise vortices generated from the plane of second expansion also dissipate by the position $z=10$. Therefore, as in the previous investigations, Fig. 2(c) demonstrates a relatively quicker process of growth of the streamwise vortices for a square jet, and they clearly have a shorter (streamwise) life span.

The streamline pattern depicted in Fig. 2(d) reveals the internal streamwise flow evolution process in further detail. It is important to note that within the channel there takes place significantly large near-wall flow recirculation extending between the plane of first expansion and the downstream exit. This upstream moving flow is partially entrained into the jet core through the dynamics of the embedded streamwise vortices and the remainder returns to the main stream upon reaching the plane of first expansion; such a physical process thereby helps to enhance mixing. Furthermore, it may be carefully noted that the process of near-wall upstream fluid motion receives not only favorable but indeed very strong support from the second expansion zone. Since the enhancement of mixing is most welcome and of major concern in the combustion industry, the streamwise flow evolution details both on the symmetry plane $y=0$ and on $y=0.49$ suggest that the existence of a second expansion in the nozzle geometry will be effective towards achieving such an objective. Since the inlet channel has unit nondimensional width, the location $y=0.49$ is suitably chosen to demonstrate the fact that, as we move closer to the wall, the width of the upstream recirculating flow increases considerably. Importantly, the structure of dotted contours of the streamwise velocity (w) presented in Fig. 2(a) clearly support such an observation. Since the developed flow remained symmetric (see also Hertzberg and Ho [6] and Sau [8]), the streamwise flow evolution details are presented only on $y=$ const planes.

B. Generation of streamwise vortices

In a couple of recent investigations concerning 3D flows through a rectangular sudden expansion and contraction, Sau [3,9] presented a pressure analysis which could successfully identify the presence of all streamwise vortices in the physical setup, and demonstrates the fact that the nonuniform flow acceleration, as induced by the developed transverse pressure gradient skewing, effectively controls the generation of the streamwise vortices. To be more precise, on every transverse sectional plane, there developed several relatively high and low pressure regions of different strength, and it has been observed that the associated flow acceleration from these high pressure regions towards the neighboring low pressure regions (due to the generated transverse pressure gradient skewing) effectively influences the generation process of the streamwise vortices. Furthermore, it has also been verified that the corresponding azimuthal dynamics (e.g., Sau [9]) of the vortices cannot induce the generation of these streamwise vortices. Since the simulated streamwise vortices in a two-step square sudden expansion flow maintained an evolution process which is relatively complex and quite different from what we observed for the asymmetric (rectangular) sudden expansion flows, our interest here is to investigate the process of generation of the streamwise vortices in the present setup and to verify whether a parallel pressure analysis can effectively detect their presence.

Interestingly, for the presently investigated square sudden expansion flow, the pressure (p) contours presented in Fig. 2(a) (column 4) reveal the development of several symmetrically formed relatively high and the low pressure regions at every z station, and the orientation of these high and the low pressure regions are seen to vary from one streamwise station to another. Fluid over a jet section is therefore expected to get accelerated accordingly from the high pressure regions to the neighboring low pressure regions. Following Sau [3,9], from each high pressure region on a transverse sectional plane we draw curved arrows so that they embrace every neighboring low pressure region in its vicinity from both sides, and the same procedure is adopted for the contours on every z station and for all the investigated cases. For example, from the developed central high pressure region on $z=0.05$ [Fig. 2(a), column 4] we draw arrows, which embrace the surrounding low pressure regions. Here we may mention that the presence of such an arrow in the computed pressure field should indicate the formation of a streamwise vortex at the region, and the clockwise or anticlockwise sense of an arrow should determine whether the developed streamwise vortex will be of negative or positive strength. It is important to note that the presence of eight arrows [Fig. 2(a), column 4] with the sectional pressure field on $z=0.05$ matches exactly with the corresponding computed streamwise dynamics for the flow [Fig. 2(a), column 2], and reveals the formation of a pair of counter rotating streamwise vorti-

ces from each inner corner on the plane of first expansion. Owing to sudden expansions of the physical geometry, the pressure distribution within the channel is seen to change with streamwise distance. One such evidence may be noted with the pressure distribution on $z=2$ [Fig. 2(a), column 4] where the orientation of the developed relatively high and the low pressure contours is seen to get twisted by 45° with respect to the principle axes. However, on $z=2$ also the predicted vorticity dynamics, as indicated by arrows with the pressure contours, is seen to match exactly with the corresponding computed streamwise dynamics of the flow [Fig. 2(a), column 3], and the nonuniform flow acceleration due to the developed transverse pressure gradient skewing presumably induces the growth of the vortices (e.g., see Zaman [2], Sau [3], Bradshaw [17]). Furthermore, the sense of the arrows with the pressure contours on $z=4$ and $z=7$, extending from the central relatively high pressure region and embracing the neighboring low pressure regions, predicts exactly the same streamwise dynamics for the flow on the corresponding planes obtained from the simulation [Fig. 2(a), column 3].

As the flow approached the second expansion zone, a substantial readjustment in the orientations of the developed pressure distribution is observed. For example, on $z=8.1$, that is, soon after the plane of second expansion, the pressure contours [Fig. 2(a), column 4] indicate the formation of a relatively low pressure region at the jet centerline and the development of four distinct high pressure regions surrounding the central low pressure area. Notably, the sense of the four pairs of inner arrows (Fig. 2, column 4) with the pressure contours on $z=8.1$ (which are directed towards the central low pressure region) corresponds to the four pairs of upstream streamwise vortices that entered into the second expansion zone from the first expansion zone and match exactly with the corresponding (Fig. 2, column 3) computed streamwise dynamics (on $z=8.1$) for the flow. Furthermore, the presence of other eight pairs of outer arrows with the pressure contours on $z=8.1$ (Fig. 2, column 4) corresponds to the four pairs of additional streamwise vortices which are generated from the four inner edges (A,B,C,D, as indicated in Fig. 1) on the plane of second expansion and the four pairs of induced wall vortices that remained attached to the surrounding walls. Interestingly, the sense and the relative position of these arrows also match exactly with the corresponding computed streamwise dynamics on $z=8.1$ [Fig. 2(a), column 3]. In particular, the observed change in the pressure distribution on $z=9$ suggests that the pressure at this location has once again readjusted itself suitably to support the dissipation of the transmitted upstream vortices and the growth of newly generated streamwise vortices. Again, the nature of depicted arrows on $z=9$ [Fig. 2(a), column 4] clearly reveals the simulated local streamwise dynamics for the flow [e.g., see Fig. 2(a), column 3]. Here we may mention that the relative arrangement of the developed high and the low pressure regions on $z=10$ remained quite similar to those on $z=9$, however, the lack of suitable space prevents us from presenting those results in further detail.

At this point it may be interesting to explore how the developed pressure gradient skewing, as revealed by Fig. 2(a) (column 4), controls the three-dimensional flow evolution over the channel and influences the transverse flow behavior. For this, in Fig. 3 we plot the streamline pattern on the corresponding sectional planes. It is important to note that, on $z=0.05$ (Fig. 3) the streamline pattern within the rectangular core region clearly indicate the possible development of four pairs of outflow type streamwise vortices situated at the four corners [Fig. 2(a), column 2] and they really correspond to the predicted transverse flow behaviour on $z=0.05$ [Fig. 2, column 4], as obtained from the pressure analysis. Again, the streamline patterns on $z=2$ display the kind of flow evolution that support the formation of both inner (those generated from the plane of first expansion) and the symmetrically placed outer (passive forcing induced wall vortices) eddies. Since the pressure on the channel boundary always remained higher, the inward stretching behavior of the streamlines (issuing from the periphery) over the channel sections (Fig. 3) suggests that the developed near-wall upstream flow, as evidenced by the dotted contours of the

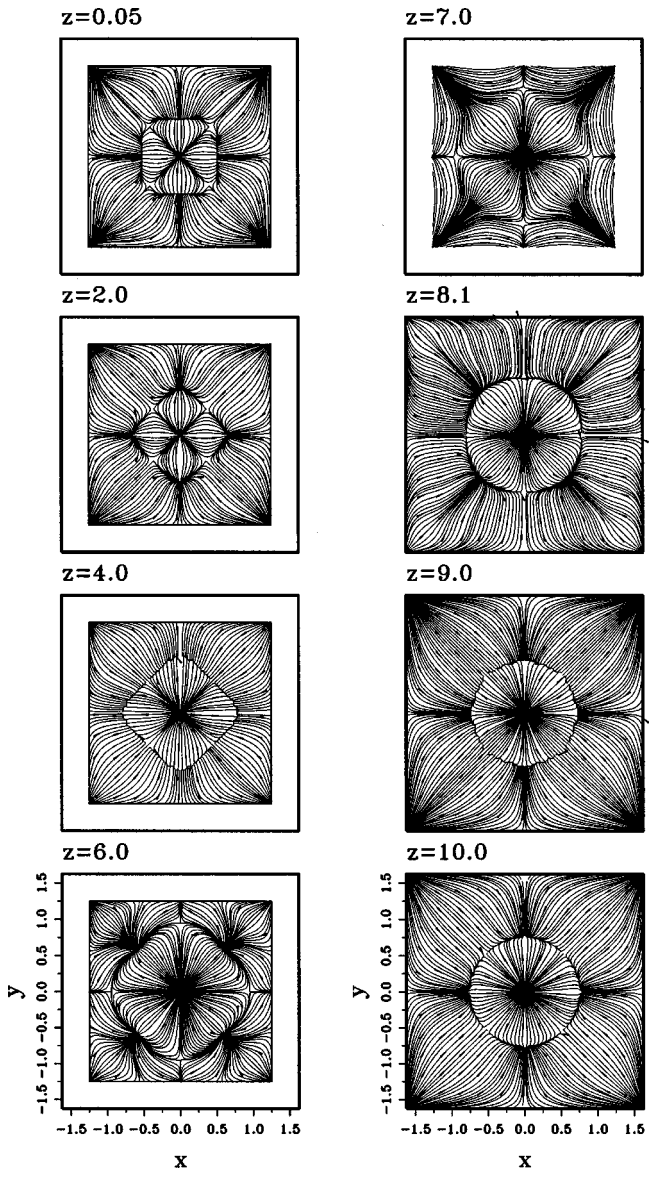

FIG. 3. Transverse flow evolution through different streamwise (z) stations at $Re=300$.

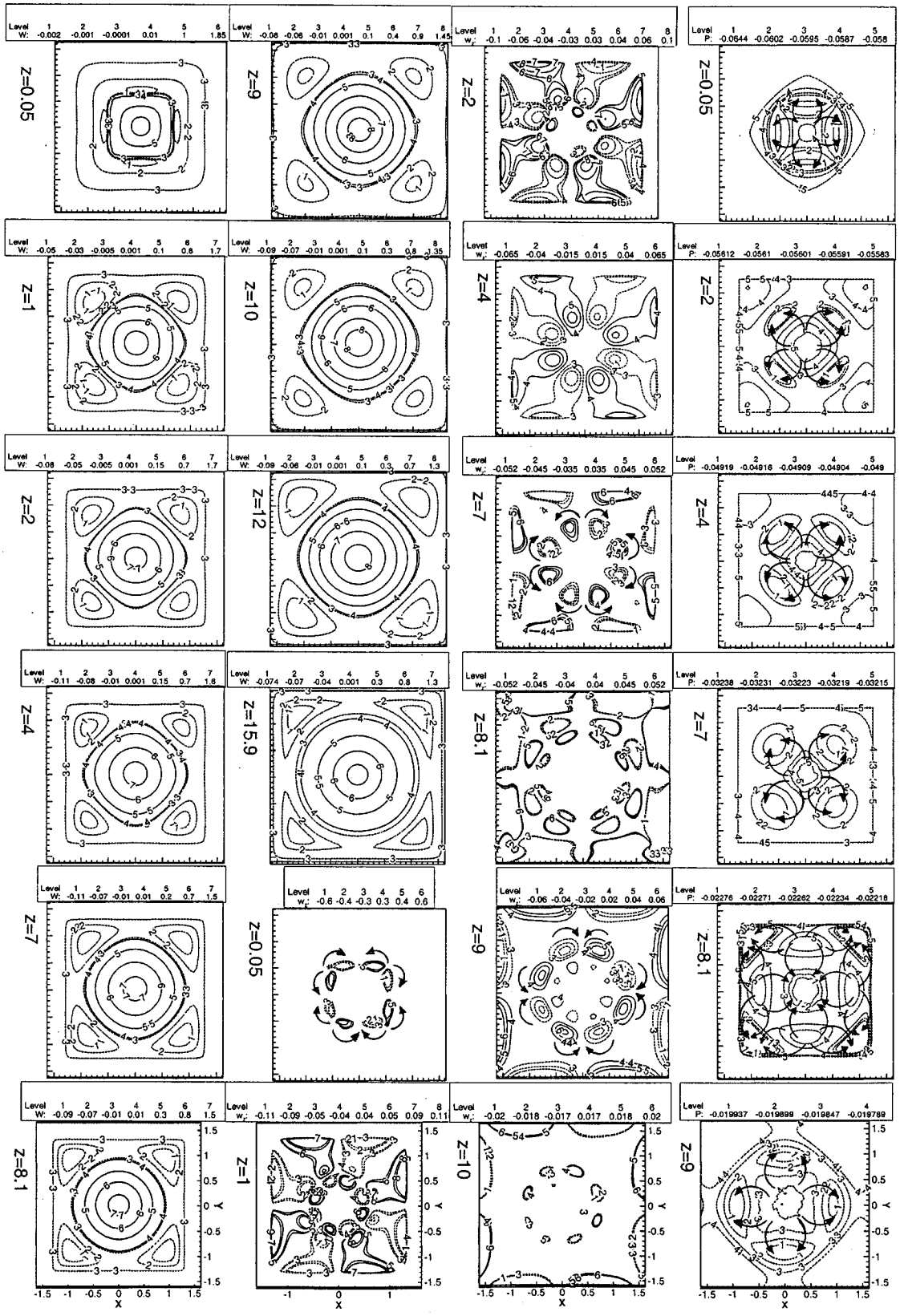

FIG. 4. Contours of the streamwise velocity (w), streamwise vorticity (ω_z) and the dynamic pressure (p) at $Re=400$.

streamwise velocity w in Fig. 2(a), and the streamwise flow recirculation in Fig. 2(d) extending over both the expansion zones, is always entrained into the jet core. Owing to the coexistence of the fast decaying core vortices and the gradually strengthening wall eddies, the governing three-dimensional flow evolution immediately behind the two planes of expansions becomes quite complex. However, for $4 \leqslant z \leqslant 7$ and $9 \leqslant z \leqslant 10$, consistency between the streamline patterns (Fig. 3), predicted streamwise dynamics from the pressure analysis [Fig. 2(a), column 4], and the corresponding computed vorticity contours [Fig. 2(a), column 3 and Fig. 2(c)] became more and more evident.

In Fig. 4 we present the flow evolution details at $Re = 400$. As in $Re = 300$, the isocontours of the streamwise (w) velocity at $Re = 400$ (Fig. 4, columns 1 and 2) reveal that immediately after entering the first expansion zone, the jet starts to expand quickly along the two principle (x and y) axes of symmetry. As a result, the jet deforms in such a way that it appears as if, in the region $1 \leqslant z \leqslant 4$, the entire jet has rotated by 45°. While the jet is seen to assume circular shape first near the second expansion zone and eventually at the channel exit, it suffered mild azimuthal perturbations (Fig. 4, column 2) between $9 \leqslant z \leqslant 12$. As far as the qualitative nature of streamwise dynamics for this flow is concerned, at every streamwise station between $0.05 \leqslant z \leqslant 9$, one observes the formation of four pairs of outflow type streamwise vortices (Fig. 4, columns 2 and 3) at the four edges of the local jet diagonals. Moreover, at this elevated Reynolds number, some relative increase in the strength of the streamwise vortices is noted. Through the outflow type dynamics, the streamwise vortices have effectively forced the jet to expand outward along the two principle planes of symmetry. It appears that the eventual dissipation of the core streamwise vortices facilitated the jet to become circular near the channel exit.

As in the previous case, the depicted pressure contours at $Re = 400$ (Fig. 4, column 4) also reveal the formation of several relatively high and low pressure regions over the flow domain, which essentially leads to the development of transverse pressure gradient skewing. Fluid over a channel section, therefore, is accelerated from the high pressure region towards the neighboring low pressure regions. Following the same convention as described before, here also from each high pressure region (on a transverse plane) we draw curved arrows embracing every existing neighboring low pressure region in its vicinity from both sides, and the same procedure is followed for the contours on every streamwise station. It is important to note that at $Re = 400$ the arrows with the pressure contours (Fig. 4, column 4) at different streamwise stations again correctly identify the presence of all the streamwise vortices in the flow, as the sense of the depicted arrows on the respective planes matches exactly with the corresponding computed streamwise dynamics for the flow, which are presented in columns 2 and 3 (Fig. 4). The observed local changes in the relative arrangements of the developed high and the low pressure regions within the channel (with respect to the principle axes), as observed between $0.05 \leqslant z \leqslant 2$ and again between $7 \leqslant z \leqslant 8.1$, clearly contribute to the associated changes in the streamwise dynamics of the flow.

V. CONCLUDING REMARKS

In the present study, the nature of evolution of a square jet through two consecutive steps of sudden expansion has been simulated numerically. Upon entering into the first expansion zone, the jet is observed to experience relatively quick azimuthal perturbations behind the plane of first expansion, where it appears to have rotated by 45° due to its rapid expansion along the two principle planes of symmetry. However, during the downstream evolution, the jet becomes circular at about six cylinder diameters behind the plane of first expansion. From the dynamics of the embedded streamwise vortices it appears that, the faster growth of the passive forcing induced wall vortices, starting immediately behind the plane of first expansion, and subsequent dominance of these vortices over the first expansion zone in the form of four outflow type pairs, with one such pair occupying its position at an end of a local jet diagonal, facilitated the quick outward spreading of the jet along the two principle planes of symmetry, leading to an apparent 45° rotation of the jet structure. Most importantly, we have established a pressure analysis which efficiently predicts the presence of all the streamwise vortices in the physical setup, and suggests that the transverse pressure gradient skewing influences the generation of these streamwise vortices. To be more precise, the transverse sectional pressure distribution through different streamwise stations indicate the formation of several relative high and the low pressure regions within the channel, which contributes to the development of transverse pressure gradient. The nonuniform flow acceleration from the developed relatively high pressure regions towards the neighboring low pressure regions is found to influence the generation of the streamwise vortices. Furthermore, the pressure analysis successfully predicts every local change in the streamwise dynamics within the physical domain, which is contributed due to the local growth of the passive forcing induced new vortices and dissipation of the preexisting upstream streamwise vortices. Such local changes in the streamwise dynamics also appear to be controlled by the local adjustment in the transverse pressure distribution.

ACKNOWLEDGMENT

The author sincerely thanks Professor Robert Hwang and Dr. W. C. Yang for their valuable help.

[1] D. Liepmann and M. Gharib, J. Fluid Mech. **245**, 643 (1992).
[2] K. B. M. Q. Zaman, J. Fluid Mech. **316**, 1 (1996).
[3] A. Sau, Phys. Fluids **14**, 3280 (2002).
[4] H. S. Husain and A. K. M. F. Hussain, Phys. Fluids **26**, 2763 (1983).
[5] C. M. Ho and E. Gutmark, J. Fluid Mech. **179**, 383 (1987).
[6] J. R. Hertzberg and C. M. Ho, AIAA J. **30**, 2420 (1992).
[7] J. R. Hertzberg and C. M. Ho, J. Fluid Mech. **289**, 1 (1995).
[8] A. Sau, Phys. Fluids **11**, 3003 (1999).
[9] A. Sau (private communication).
[10] M. P. duPlessis, R. L. Wang, and R. Kahawita, J. Fluids Eng. **96**, 246 (1974).
[11] W. R. Quinn and J. Militzer, Phys. Fluids **31**, 1017 (1988).
[12] W. R. Quinn, AIAA J. **30**, 2852 (1992).
[13] F. F. Grinstein, E. Gutmark, and T. Parr, Phys. Fluids **7**, 1483 (1995).
[14] F. F. Grinstein and C. R. DeVore, Phys. Fluids **8**, 1237 (1996).
[15] D. O. Davis and F. B. Gessner, AIAA J. **30**, 367 (1992).
[16] J. J. Miau, T. S. Leu, J. H. Chou, S. A. Lin, and C. K. Lin, AIAA J. **28**, 1447 (1990).
[17] P. Bradshaw, Annu. Rev. Fluid Mech. **19**, 53 (1987).
[18] J.-H. Kim and M. Samimy, Phys. Fluids **11**, 2731 (1999).
[19] F. M. White, *Viscous Fluid Flows*, 2nd ed. (McGraw-Hill, New York, 1991).
[20] A. Sau, R. R. Hwang, T. W. Sheu, and W. C. Yang, Phys. Rev. E **68**, 056303 (2003).
[21] F. H. Harlow and C. H. Welch, Phys. Fluids **8**, 2182 (1965).
[22] T. P. Chiang, T. W. H. Sheu, R. R. Hwang, and A. Sau, Phys. Rev. E **65**, 016306 (2002).
[23] A. Sau and A. K. Lahiri, Acta Mech. **124**, 79 (1997).
[24] Y. F. Peng, Y. H. Shiau, and R. Hwang, Comput. Fluids **32**, 337 (2003).